

# Bacterial Community Reconstruction Using A Single Sequencing Reaction

Amnon Amir<sup>1,\*</sup> Or Zuk<sup>2,\*</sup>

October 15, 2018

## Abstract

Bacteria are the unseen majority on our planet, with millions of species and comprising most of the living protoplasm. While current methods enable in-depth study of a small number of communities, a simple tool for breadth studies of bacterial population composition in a large number of samples is lacking. We propose a novel approach for reconstruction of the composition of an unknown mixture of bacteria using a single Sanger-sequencing reaction of the mixture. This method is based on compressive sensing theory, which deals with reconstruction of a sparse signal using a small number of measurements. Utilizing the fact that in many cases each bacterial community is comprised of a small subset of the known bacterial species, we show the feasibility of this approach for determining the composition of a bacterial mixture. Using simulations, we show that sequencing a few hundred base-pairs of the 16S rRNA gene sequence may provide enough information for reconstruction of mixtures containing tens of species, out of tens of thousands, even in the presence of realistic measurement noise. Finally, we show initial promising results when applying our method for the reconstruction of a toy experimental mixture with five species. Our approach may have a potential for a practical and efficient way for identifying bacterial species compositions in biological samples.

Availability: A MATLAB code is available at:

[http://www.broadinstitute.org/~orzuk/matlab/libs/BCS/matlab\\_BCS\\_utils.html](http://www.broadinstitute.org/~orzuk/matlab/libs/BCS/matlab_BCS_utils.html)

## 1 Introduction

Microorganisms are present almost everywhere on earth. The population of bacteria found in most natural environments consists of a large number of species, mutually affecting each other, and creating complex ecological systems [38]. In the human body, the number of bacterial cells is over an order of magnitude larger than the number of human cells [49], with typically several hundred species identified in a given sample taken from humans (for example, over 400 species were characterized in the human gut [24], while [51] estimates a higher number of 500-1000, and 500 to 600 species were found in the oral cavity [19, 48]). Changes in the human bacterial community composition are associated with physical condition, and may indicate [43] as well as cause or prevent various microbial

---

<sup>1</sup>Department of Physics of Complex Systems, The Weizmann Institute of Science, Rehovot, Israel

<sup>2</sup>Broad Institute of MIT and Harvard, Cambridge, Ma, USA

\*Equal contribution

diseases [31]. In a broader aspect, studies of bacterial communities range from understanding the plant-microbe interactions [53], to temporal and meteorological effects on the composition of urban aerosols [7], and is a highly active field of research [46].

Identification of the bacteria present in a given sample is not a simple task, and technical limitations impede large scale quantitative surveys of bacterial community compositions. While conventional phenotypic methods (such as fatty acid profiles, carbon source utilization and biochemical identification) are relatively inexpensive, they often show an inaccurate and biased identification [15, 57]. Such methods were shown to provide incorrect identification of many organisms (see [5, 54]), and additionally rely on the availability of pure culture of each bacteria present in the sample. Since the vast majority of bacterial species are non-amenable to standard laboratory cultivation procedures [1], this leads to a highly biased identification. Much attention has been therefore given to alternative, culture-independent methods. The golden standard of microbial population analysis has been direct Sanger sequencing of the ribosomal 16S subunit gene (16S rRNA) [35]. Briefly, DNA from the bacterial population is extracted and PCR amplified using universal primers. The resulting 16S rRNA gene is cloned and single colonies are sequenced using Sanger sequencing. This method offers high accuracy since the whole 16S rRNA gene is sequenced and used for identification of each clone. However, the sensitivity of this method is determined by the number of sequencing reactions, and therefore requires hundreds of sequences for each sample analyzed. Due to the high cost and labor of such a process, using this method is limited to in-depth study on a small number of samples (see for example [24]). A modification of this method for identification of small mixtures of bacteria using a single Sanger sequence has been suggested [39] and showed promising results when reconstructing mixtures of 2-3 bacteria from a given database of 260 human pathogen sequences.

Recently, DNA microarray-based methods [30] and identification via next generation sequencing (reviewed in [33]) have been used for bacterial community reconstruction. In microarray based methods, such as the Affymetrix PhyloChip platform [7], the sample 16S rRNA is hybridized with short probes aimed at identification of known microbes at various taxonomy levels. While being more sensitive and cheaper than standard cloning and sequencing techniques, each bacterial mixture sample still needs to be hybridized against a microarray, thus the cost of such methods limit their use for wide scale studies. While most microarray-based methods require a design of arrays with a different probe specific to each one of the species to be detected, a recent approach [16] has proposed to use universal Compressed-Sensing based microarray design, in which one takes into account the hybridization of a given probe to multiple (rather than single) different sequences. Methods based on next generation sequencing obtain a very large number of reads of a short hyper-variable region of the 16S rRNA [2, 18, 34]. By matching these sequence reads to known 16S rRNA sequences, the bacterial composition is reconstructed. Usage of such methods, combined with DNA barcoding, enables high throughput identification of bacterial communities, and can potentially detect species present at very low frequencies. However, since such sequencing methods are limited to relatively short read lengths (typically a few dozens and at most a few hundred bases in each sequence), the identification is non unique and limited in resolution, with reliable identification typically up to the genus level [36]. Improving the resolution depends on obtaining longer read lengths, which is currently technologically challenging.

In this work we suggest a novel experimental and computational approach for sequencing-based profiling of bacterial communities (see Figure 1.1). Our method relies on a single Sanger sequencing reaction for a bacterial mixture, which results in a linear combination of the constituent sequences. Using this mixed chromatogram as linear constraints, the sequences which constitute the original

mixture are selected using a Compressed Sensing (CS) framework.

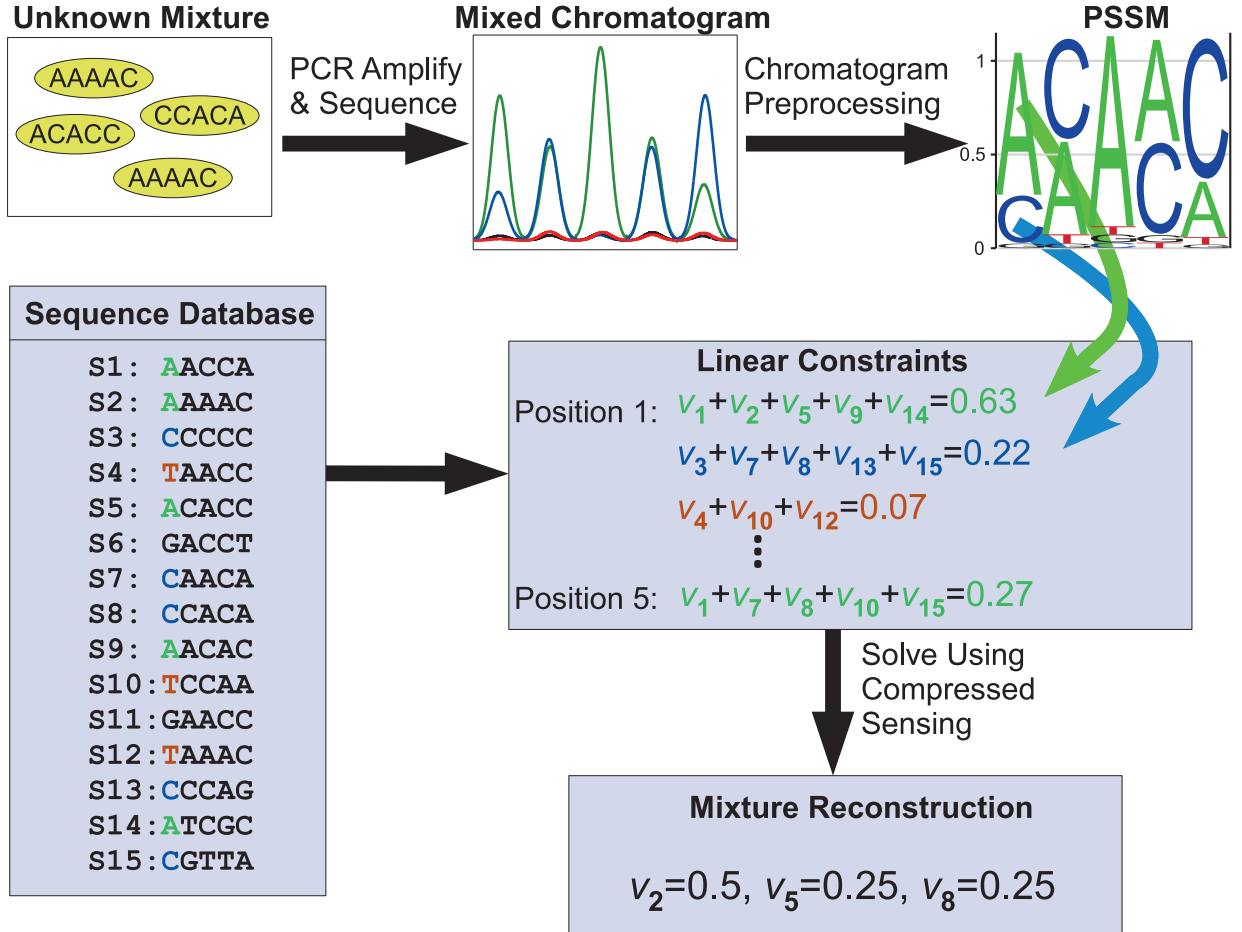


Figure 1.1: **Schematics of the proposed BCS reconstruction method.** The 16S rRNA gene is PCR-amplified from the mixture and then subjected to Sanger sequencing. The resulting chromatogram is preprocessed to create the Position Specific Score Matrix (PSSM). For each sequence position, four linear mixture equations are derived from the 16S rRNA sequence database, with  $v_i$  denoting the frequency of sequence  $i$  in the mixture, and the frequency sum taken from the experimental PSSM. These linear constraints are used as input to the CS algorithm, which returns the sparsest set of bacteria recreating the observed PSSM.

Compressed Sensing (CS) [8, 20] is an emerging field of research, based on statistics and optimization with a wide variety of applications. The goal of CS is recovery of a signal from a small number of measurements, by exploiting the fact that most natural signals (e.g. natural images or human speech) are in fact sparse, or approximately sparse, when represented at a certain appropriate basis. Compressed Sensing designs sampling techniques that condense the information of a compressible signal into a small amount of data. This offers the possibility of performing fewer measurements

than were thought to be needed before, thus lowering costs and simplifying data-acquisition methods for various types of signals in many distantly related fields such as magnetic resonance imaging [42], single pixel camera [23], geophysics [40] and astronomy [4].

**CS** was recently applied to various problems in computational biology, e.g. for pooling designs for re-sequencing experiments [25, 52], and for drug-screenings [37]. Lately **CS** was also used to design multiplexed DNA microarrays [16], where each spot is a combination of several different probes. By specific selection and mixing of the probes, a **CS** microarray was designed for detection of bacterial species in a community using a small number of probe spots.

The classical problem in **CS** is solving an under-determined linear system of equations

$$\mathcal{A}\mathbf{v} = \mathbf{b} \tag{1.1}$$

where  $\mathbf{v} = (v_1, \dots, v_N)$  is the vector of unknown variables,  $\mathcal{A}$  is the *sensing* matrix, often called also the *mixing* matrix and  $\mathbf{b} = (b_1, \dots, b_k)$  are the measured values of the  $k$  equations. The number of variables  $N$ , is far greater than the number of equations  $k$ . Without further information,  $\mathbf{v}$  cannot be reconstructed uniquely since the system is under-determined. Here one uses an additional sparsity assumption on the solution - by assuming that we are interested only in solution vectors  $\mathbf{v}$  with only at most  $s$  non-zero entries, for some  $s \ll N$ . According to the **CS** theory, when the matrix  $\mathcal{A}$  satisfy certain conditions, most notably the RIP condition [10, 12], one can find the sparsest solution uniquely by using only a logarithmic number of equations,  $k = O(s \log(N/s))$ , instead of a linear number ( $N$ ) needed for general solution of a linear system. Furthermore, efficient algorithms exist which make finding the solution practical even for very large sensing matrices, with  $N$  sizes up to tens of thousands of variables. Intuitively, the RIP condition states that the columns of the matrix  $A$  are not similar to each other, and in fact close to orthogonal. More details on the requirements from the matrix  $A$ , the problem representation and algorithms for solutions of **CS** problems are given in the Methods section, as well as in the aforementioned references.

In this paper, we show an efficient application of pooled Sanger-sequencing for reconstruction of bacterial communities using **CS**. The sparseness assumption in our scenario is obtained by noting that although numerous species of bacteria have been characterized and are present on earth, at a given sample typically only a small fraction of them are present at significant levels, while the proportion of all other species is essentially zero. This assumption enables an accurate reconstruction of the non-zero frequencies, from a relatively small amount of information, obtained by a single sequence of a certain gene such as the 16S rRNA gene. The proposed Bacterial Compressed Sensing algorithm (**BCS**) uses as inputs a database of known 16S rRNA sequences and the measured Sanger-sequence of the unknown mixture, and returns the sparse set of bacteria present in the mixture and their predicted frequencies. The measured Sanger-sequence we use as input comes as a chromatogram, representing a linear combination of DNA sequences coming from species in our mixture. This is different from the commonly used chromatograms which typically represent a single sequence. We therefore developed a set of pre-processing steps adjusted for such mixed chromatograms - the use of these steps, before applying the **CS** optimization procedure, was crucial for the success of the reconstruction. We show a successful reconstruction of simulated mixtures containing dozens of bacterial species out of a database of tens of thousands, using realistic biological parameters. In addition, we demonstrate the applicability of our proposed method for a real sequencing experiment using a toy mixture of five bacterial species.

## 2 Methods

### 2.1 The Bacterial Community Reconstruction Problem

In the Bacterial Community Reconstruction Problem we are given a bacterial mixture of unknown composition. In addition, we have at hand a database of the orthologous genomic sequences for a specific known gene, which is assumed to be present in a large number of bacterial species (in our case, the gene used was the 16S rRNA gene). Our purpose is to reconstruct the identity of species present in the mixture, as well as their frequencies, where the assumption is that the sequences for the gene in all or the vast majority of species present in the mixture are available in the database. The data used for the reconstruction problem is obtained from sequencing the specific gene in the bacterial mixture. The input to the reconstruction algorithm is thus the measured Sanger sequence of the gene in the mixture (see Figure 1.1). We used the 16S rRNA gene for reconstruction for two reasons: first, its sequence is known for a very large number of bacteria, and databases with these sequences are available [17, 44]. Second, the gene contains both several highly conserved regions as well as variable regions. The conserved regions can serve for universal amplification and sequencing of the gene using a single primer. The sequence information from the variable regions provides the ability to distinguish between the different species present in the mixture. Since Sanger sequencing proceeds independently for each DNA strand present in the sample, the sequence chromatogram of the mixture corresponds to the linear combination of the constituent sequences, where the linear coefficients are proportional to the abundance of each species in the mixture. Using this mixture sequence as linear constraints on the bacterial mixture composition, we try to determine the composition of the mixture.

Let  $N$  be the number of known bacterial species present in our database. Each bacterial population is characterized by a vector  $\mathbf{v} = (v_1, \dots, v_N)$  of frequencies of the different species. Denote by  $s$  the number of species present in the sample  $s = \|\mathbf{v}\|_{\ell_0}$ , where  $\|\cdot\|_{\ell_0}$  denotes the  $\ell_0$  norm which simply counts the number of non-zero elements of a vector  $\|\mathbf{v}\|_{\ell_0} = \sum_i 1_{\{v_i \neq 0\}}$ . While the total number of known species  $N$  is usually very large (in our case on the order of tens to hundreds of thousands), a typical bacterial community consists of a small subset of the species, and therefore in a given sample,  $s \ll N$ , and  $\mathbf{v}$  is a sparse vector. The database sequences are denoted by a matrix  $S$ , where  $S_{ij}$  is the  $j$ 'th nucleotide in the orthologous sequence of the  $i$ 'th species ( $i = 1, \dots, N, j = 1, \dots, k$ ). We represent the results of the mixture Sanger sequencing of length  $k$  as a  $4 \times k$  Position-specific-Score-Matrix (PSSM)

$$P = \begin{pmatrix} a_1 & a_2 & \cdots & a_k \\ c_1 & c_2 & \cdots & c_k \\ g_1 & g_2 & \cdots & g_k \\ t_1 & t_2 & \cdots & t_k \end{pmatrix} = \begin{pmatrix} \mathbf{a} \\ \mathbf{c} \\ \mathbf{g} \\ \mathbf{t} \end{pmatrix} \quad (2.1)$$

where  $\mathbf{p}_j = (a_j, c_j, g_j, t_j)^t$  is a column vector representing the observed frequencies at sequence position  $j$  of the four nucleotides, with  $a_j, c_j, g_j, t_j \geq 0$ .

Each position in the mixed sequence gives information about the bacterial composition of the mixture. For example, if at a certain position  $j$ , the frequency  $a_j$  of 'A' in the mixed sequence is 0, and assuming no measurement noise is present, it follows that all bacteria which have 'A' at the  $j$ 'th position of their orthologous gene are not present in the mixture. More generally, the frequency of each nucleotide at a given position  $j$  gives a linear constraint on the mixture:

$$\sum_{i=1}^N v_i 1_{\{S_{ij}='A'\}} = a_j \quad (2.2)$$

and similarly for 'C', 'G', 'T'.

Define the  $k \times N$  mixture matrix  $A$  for the nucleotide 'A':

$$A_{ij} = \begin{cases} 1 & S_{ij} = 'A' \\ 0 & \text{otherwise} \end{cases} \quad (2.3)$$

and similarly for the nucleotides 'C', 'G', 'T'. The constraints given by the sequencing reaction can therefore be expressed as:

$$A\mathbf{v} = \mathbf{a}, C\mathbf{v} = \mathbf{c}, G\mathbf{v} = \mathbf{g}, T\mathbf{v} = \mathbf{t} \quad (2.4)$$

Hence, from a single sequencing reaction of length  $k$  we derive a set of  $4k$  linear equations. Since a typical sequencing reaction is of length  $k \sim 500 - 1000$ , the total number of equations is  $4k \sim 2000 - 4000$ . This is still considerably smaller than the number of free variables  $N$  which is on the order of tens to hundreds of thousands. Hence, this is an underdetermined linear system, and without further assumptions we are not guaranteed a single solution. The crucial assumption we make in order to cope with the insufficiency of information is the sparsity of the vector  $\mathbf{v}$ , which reflects the fact that only a small number of species are present in the mixture. This assumption enables us to formulate and solve the reconstruction as a **CS** problem, as described in the next section.

## 2.2 Mapping the Problem to Compressed Sensing - the BCS Algorithm

We seek a sparse solution for the set of equations (2.4). Such a solution provides a small set of species which is consistent with the measured data. In the **CS** paradigm, one can formulate the quest for the sparsest solution satisfying the given set of linear constraints as follows:

$$\mathbf{v}^* = \underset{\mathbf{v}}{\operatorname{argmin}} \|\mathbf{v}\|_{\ell_0} \quad \text{s.t.} \quad A\mathbf{v} = \mathbf{a}, C\mathbf{v} = \mathbf{c}, G\mathbf{v} = \mathbf{g}, T\mathbf{v} = \mathbf{t} \quad (2.5)$$

The formulation above can be easily seen as a **CS** problem - one can in principle construct a big 'sensing' matrix  $\mathcal{A}_{4k \times N}$  as a simple concatenation of the matrices A,C,G,T, and similarly a measurements vector  $\mathbf{b}$  as a concatenation of the measurements  $\mathbf{a}, \mathbf{c}, \mathbf{g}$  and  $\mathbf{t}$ , and with these notations problem (2.5) is in fact reduced to the classic **CS** problem [8] of finding the sparsest solution for eq. (1.1). From a practical point of view, problem (2.5) is known to be in general NP-Hard [11], and hence finding the optimal solution is not computationally feasible. A main cause for the hardness of the problem is the non-convex  $\ell_0$  constraint. However, a remarkable breakthrough of the **CS** theory shows that under certain conditions on the mixture matrix and the number of measurements (see below), the sparse solution can be recovered uniquely by solving a convex relaxation of the problem, which is obtained by replacing the  $\ell_0$  norm with the "closest" convex  $\ell_p$  norm, namely the  $\ell_1$  norm, leading to the following minimization problem [13, 21, 56]:

$$\mathbf{v}^* = \underset{\mathbf{v}}{\operatorname{argmin}} \|\mathbf{v}\|_{\ell_1} = \underset{\mathbf{v}}{\operatorname{argmin}} \sum_{i=1}^N |v_i| \quad \text{s.t.} \quad A\mathbf{v} = \mathbf{a}, C\mathbf{v} = \mathbf{c}, G\mathbf{v} = \mathbf{g}, T\mathbf{v} = \mathbf{t} \quad (2.6)$$

which is a convex optimization problem whose solution can be obtained in polynomial time. The above formulation requires our measurements to be precisely equal to their expected value based on the species frequency and the linearity assumption for the measured chromatogram. This description ignores the effects of noise, which is typically encountered in practice, on the reconstruction. Clearly, measurements of the signal mixtures suffer from various types of noise and biases. Fortunately, the **CS** paradigm is known to be robust to measurement noise [10, 14]. One can cope with noise by

enabling a trade-off between sparseness and accuracy in the reconstruction merit function, which in our case is formulated as:

$$\mathbf{v}^* = \underset{\mathbf{v}}{\operatorname{argmin}} \frac{1}{2} (\|\mathbf{a} - A\mathbf{v}\|_{\ell_2}^2 + \|\mathbf{c} - C\mathbf{v}\|_{\ell_2}^2 + \|\mathbf{g} - G\mathbf{v}\|_{\ell_2}^2 + \|\mathbf{t} - T\mathbf{v}\|_{\ell_2}^2) + \tau \|\mathbf{v}\|_{\ell_1} \quad (2.7)$$

This problem represents a more general form of eq. (2.6), and accounts for noise in the measurement process. This is utilized by insertion of an  $\ell_2$  quadratic error term. Importantly, even with the addition of the  $\ell_2$  term the problem (2.7) is still a convex optimization problem. The parameter  $\tau$  determines the relative weight of the error term vs. the sparsity promoting term. Increasing  $\tau$  leads to a sparser solution, at the price of a worse fit for the measurement equations, whereas decreasing  $\tau$  leads to a better fit to the equations, while possibly requiring more non-zero elements in the solution (for low enough values of  $\tau$  we can fit the equations in (2.6) precisely, and the  $\ell_2$  error term vanishes, thus the problem is reduced back to eq. (2.6)). Many algorithms which enable an efficient solution of problem (2.7) are available, and we have chosen the widely used GPSR algorithm described in [28]. The error tolerance parameter was set to  $\tau = 10$  for the simulated mixture reconstruction, and  $\tau = 100$  for the reconstruction of the experimental mixture. These values achieved a rather sparse solution in most cases (a few species reconstructed with frequencies above zero), while still giving a good sensitivity. The performance of the algorithm was quite robust to the specific value of  $\tau$  used, and therefore further optimization of the results by fine tuning  $\tau$  was not followed in this study. Accuracy of solution was evaluated using two measures, Root-Mean-Squared-Error (RMSE) and recall/precision. For the latter measure we have set a minimal frequency threshold for inclusion in both the true and the reconstructed solutions. More detailed are provided in the Results section.

In classical **CS** one designs the mixing matrix to have certain desirable properties in order to enable unique reconstruction. The most well-known condition for successful reconstruction is the 'Robust Isometry Property' (RIP), also known as the 'Uniform Uncertainty Principle' (UUP) [10, 12]. Briefly, RIP for a matrix means that any subset of  $2s$  columns of the matrix  $\mathcal{A}$  is 'almost orthogonal' (although since  $k < N$  the columns cannot be perfectly orthogonal). This property makes the matrix  $\mathcal{A}$  'invertible' for sparse vectors  $v$  with sparsity  $s$ . Furthermore, it is known that with very high probability a unique and accurate reconstruction is achievable with as few as  $O(s \log(N/s))$  measurements, compared to  $O(N)$  measurements required for finding a solution for a general linear system without a sparsity assumption [8, 20]. In our case the number of measurements  $4k$  is on order of a few thousands, thus these results suggest that accurate reconstruction is possible, at least when the sparsity  $s$  in the range of a few dozens. One important difference between classical **CS** and our problem is the structure of the mixing matrix  $\mathcal{A}$ . In our application the mixing matrix represents the sequence database  $S$  which is pre-determined. Moreover, for species which are close in the bacterial phylogeny, the gene sequences in the database exhibit high sequence similarity and therefore the corresponding columns in the sensing matrix are far from orthogonal. It is thus far from clear in advance that the given mixing matrix posses the desired properties to enable successful reconstruction. This point is addressed in the Results section.

### 2.3 Ribosomal DNA Database

16S rRNA gene sequences were obtained from greengenes ([greengenes.1bl.gov](http://greengenes.1bl.gov)) using database version 06-2007 [17], which contains approximately 136000 chimera checked full length sequences. Sequences were reverse complemented and aligned with primer 1510R [29], resulting in approximately 42000 sequences matching the primer sequence (with up to 6 mismatches with the primer). Out of

this set, sequences with up to 2 base-pair difference with another sequence in the database were removed, resulting in  $N = 18747$  unique sequences which were used in this study. This last step was used in order to reduce the size of the input to the GPSR algorithm, thus enabling solution of the **CS** problem using a standard PC.

The sequence of *Enterococcus faecalis* (ATCC # 19433) was manually added to the list of unique sequences, as it did not appear in the database (closest neighbor in the database has 32 different positions), and is used in the experimental mixture.

## 2.4 Experimental Mixture Reconstruction

### 2.4.1 Sample Preparation

Strains used for the experimental reconstruction were: *Escherichia coli* W3110, *Vibrio fischeri*, *Staphylococcus epidermidis* (ATCC # 12228), *Enterococcus faecalis* (ATCC # 19433) and *Photobacterium leiognathi*. The 16S rRNA gene was obtained from each bacterial strain by boiling for one minute followed by 40 cycles of PCR amplification. Primers used for the PCR were the universal primers 8F and 1510R [29], amplifying positions 8-1513 of the *E. coli* 16S rRNA:

**8F:** 5'-AGAGTTTGTATYMTGGCTCAG

**1510R:** 5'-TACGGYTACCTTGTTACGACTT

For mixture preparation and sequencing, equal amounts of DNA from each bacterial 16S rRNA gene were mixed together, and then sequenced using an ABI3730 DNA Analyzer (Applied Biosystems, USA) using the 1510R primer.

### 2.4.2 Preprocessing Steps

The input to the **BCS** algorithm is a  $4 \times k$  PSSM  $(\mathbf{a}, \mathbf{c}, \mathbf{g}, \mathbf{t})^t$  of the mixture. However, obtaining this PSSM from an experimental mixture is not trivial. The output of a Sanger-sequencing reaction is a chromatogram, which describes the fluorescence of the four terminal nucleotides as a function of sequence position. In classical single-species sequencing, each peak in the chromatogram corresponds to a single nucleotide in the sequence. Identifying the peaks becomes more complicated when sequencing a mixture of different sequences. It has been previously shown (see e.g. [6, 47]) that chromatogram peak height and position depend on the local sequence of nucleotides preceding a given nucleotide. Therefore, when performing Sanger sequencing of a mixture of multiple DNA sequences, the peaks of the constituent sequences may lose their coherence, making it nearly impossible to determine where the chromatogram peaks are located. We therefore opted for a slightly different approach for preprocessing of the chromatogram, which does not depend on identifying the peak for each nucleotide. Rather, the chromatogram is binned into constant sized bins, and the total intensity of each of the four nucleotides in each bin is used to construct the PSSM used as input to the **BCS** (see Figure A.1.A). A similar process is applied to each sequence in the 16S rRNA database. In order to correct for local-sequence effects, statistics were collected for local-sequence dependence of peak height and position. Similar statistics are used to obtain quality scores for single-sequence chromatogram base-calling in the Phred algorithm [26, 27]. By utilizing these statistics, we predict the chromatogram for each sequence in the database, which is then binned and results in a PSSM for the single sequence. This database of predicted PSSMs is then used to construct the mixing matrices  $A, C, G, T$  participating in the **BCS** problem representation in eq. (2.7) (see Figure A.1.B). The details of the preprocessing steps for the database sequences and the measured chromatogram are



given in the appendix.

## 3 Results

### 3.1 Simulation Results

In order to assess the performance of the proposed **BCS** reconstruction algorithm, random subsets of species from the greengene database [17] were selected. Within these subsets, the relative frequencies of each species were drawn at random from a uniform frequency distribution (normalized to sum to one), and a mixed sequence PSSM was calculated (results for a different, power-law frequency distribution, are shown later). This PSSM was then used as the input for the **BCS** algorithm, which returned the frequencies of database sequences predicted to participate in the mixture (see Methods section and Figure 1.1).

A sample of a random mixture of 10 sequences, and a part of the corresponding mixed sequence PSSM, are shown in Figure 3.1.A,B respectively. Results of the **BCS** reconstruction using a 500 bp long sequence are shown in Figure 3.1.C. The **BCS** algorithm successfully identified all of the species present in the original mixture, as well as several false positives (species not present in the original mixture). The largest false positive frequency was 0.01, with a total fraction of 0.04 false positives. In order to quantify the **BCS** algorithm’s performance, we used two main measures: RMSE and recall/precision. RMSE is the Root-Mean Squared-Error between the original mixture vector and the reconstructed vector, defined as  $RMSE = \|\mathbf{v} - \mathbf{v}^*\|_{\ell_2} = \left(\sum_{i=1}^N (v_i - v_i^*)^2\right)^{1/2}$ . This measure accounts both for the presence or absence of species in the mixture, as well as their frequencies. In the example shown in Figure 3.1 the RMSE score of the reconstruction was 0.03. As another measure, we have recorded the *recall*, defined as the fraction of species present in the original vector  $\mathbf{v}$  which were also present in the reconstructed vector  $\mathbf{v}^*$  (this is also known as sensitivity), and the *precision*, defined as the fraction of species present in the reconstructed vector  $\mathbf{v}^*$  which were also present in the original mixture vector  $\mathbf{v}$ . Since the predicted frequency is a continuous variable, whereas the recall/precision relies on a binary categorization, a minimal threshold for calling a species present in the reconstructed mixture was used before calculating the recall/precision scores.

#### 3.1.1 Coherence of Database Sequences

As explained in the Methods section, for successful reconstruction using a small number of measurements, the columns of the mixing matrix need to be incoherent, i.e. close to orthogonal, in accordance with the RIP condition [9]. In our case this cannot be achieved, as we were given the sequences determining the mixing matrix and cannot control them. Even though the sequences are orthologous and thus quite similar, insertions and deletions came to our aid, as they bring similar sequences to being out of phase (for example, even a deletion of a single base from a sequence, reduces its correlation with a copy of itself from one to a number typically much lower). It has been previously shown [3, 56] that a computationally feasible method for assessing the information content of the mixing matrix is the mutual coherence, defined as the maximal coherence (inner product) between two columns of the mixing matrix. The distribution of coherence values for random pairs of database species is shown in Figure 3.2. While most correlations are centered around 0.25, there exists a small fraction of highly correlated sequences, with 0.005 of the sequence pairs showing a correlation above 0.8, and a maximal correlation value of 0.998. This high mutual coherence value places a limit on the recon-

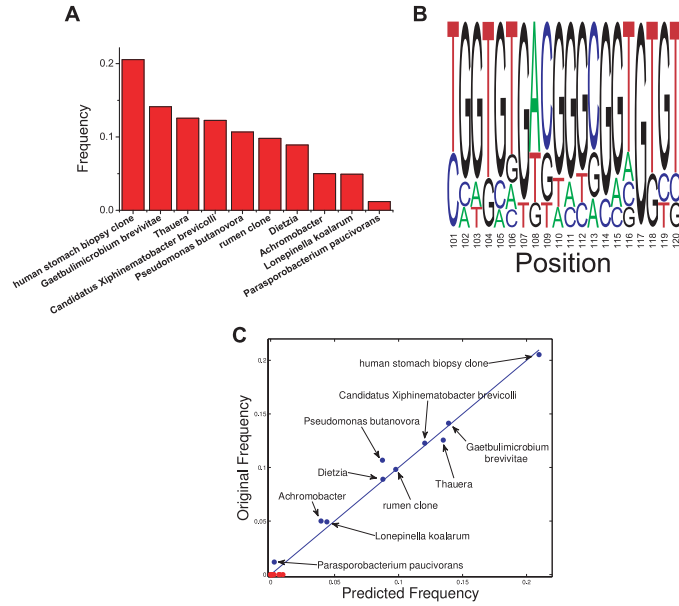


Figure 3.1: **Sample reconstruction of a simulated mixture.** **A.** Frequencies and species for a simulated random mixture of  $s = 10$  sequences. Species were randomly selected from the 16S rRNA database, with frequencies generated from a uniform distribution. **B.** A 20 nucleotide sample region of the PSSM for the mixture in (A). **C.** True vs. predicted frequencies for a sample **BCS** reconstruction for the mixture in (A) using  $k = 500$  bases of the simulated mixture. Red circles denote species returned by the **BCS** algorithm which are not present in the original mixture.

struction performance in the worst case, when such a sequence is present in the mixture. Since the database contains another highly similar sequence, distinguishing between these two is very difficult, and therefore the **CS** reconstruction cannot guarantee complete accuracy. However, given that such similar sequences are typically of closely related species (thus not being able to distinguish between them may be considered acceptable), and since most of the sequences show near random coherence, the reconstruction in most of the cases may still require only a small number of measurements (which translates into a small number of nucleotides read in the sequencing).

### 3.1.2 Effect of Sequence Length

To determine the typical sequence length required for reconstruction, we tested the **BCS** algorithm performance using different sequence lengths. In Figure 3.3.A (black line) we plot the RMSE of reconstruction for random mixtures of 10 species. To enable faster running times, each simulation used a random subset of  $N = 5000$  sequences out of the sequence database for mixture generation and reconstruction. It is shown in Figure 3.3.A that using longer sequence lengths results in a larger number of linear constraints and therefore higher accuracy, with  $\sim 300$  nucleotides sufficing for accurate reconstruction of a mixture of 10 sequences. The large standard deviation is due to a small probability of selection of a similar but incorrect sequence in the reconstruction, which leads to a

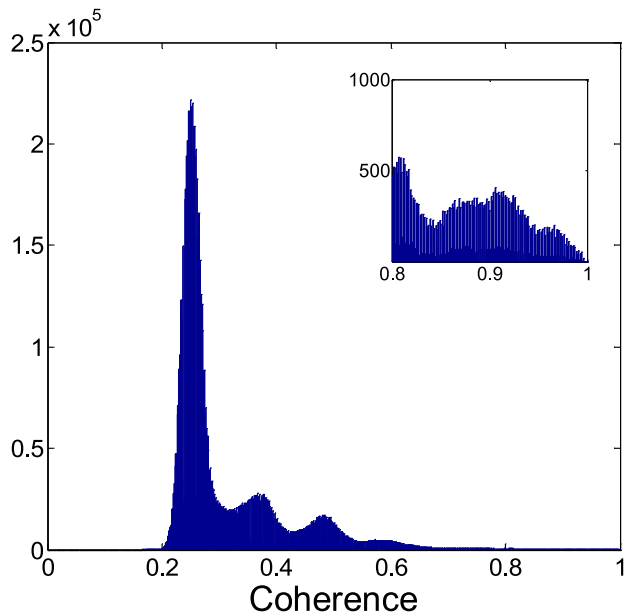


Figure 3.2: **Coherence distribution of the 16S rRNA sequences.** Coherence (inner product) of  $10^7$  16S rRNA vector pairs chosen randomly from the sequence database ( $\sim 5.7\%$  of all possible pairs). As each column of the mixture matrix is a binary vector with  $1/4$  of the coordinates being one, the dot product between two randomly generated vectors is expected to be  $\sim 0.25$ . While most 16S rRNA database pairs exhibit a coherence around 0.25, many pairs exhibit significantly higher correlations, with a few ( $\sim 0.5\%$ ) even exceeding 0.8 (see inset).

high RMSE. Due to a cumulative drift in the chromatogram peak position prediction, typical usable experimental chromatogram lengths are in the order of  $k \sim 500$  bases rather than the  $\sim 1000$  bases usually obtained when sequencing a single species (see Methods section for details).

In order to assess the effect of the dependence between the database sequences (which leads to high coherence of the mixing matrix columns) on the performance of the **BCS** algorithm, a similar mixture simulation was performed using a database of random nucleotide sequences (i.e. each sequence was composed of i.i.d. nucleotides with 0.25 probability for 'A', 'C', 'G' or 'T'). Since sequences were independently drawn, the pairwise correlation values are centered around 0.25, with maximal coherence value less than 0.4 over all pairs we have simulated (data not shown). Using a mixing matrix derived from these random sequences, the **BCS** reconstruction algorithm showed better performance (green line in Figure 3.3.A), with  $\sim 100$  nucleotides sufficing for a similar RMSE as that obtained for the 16S rRNA database using 300 nucleotides.

### 3.1.3 Effect of Number of Species

For a fixed value of  $k = 500$  nucleotides per sequencing run, the effect of the number of species present in the mixture on reconstruction performance is shown in Figure 3.3.B,C. Even on a mixture of 100 species, the reconstruction showed an average RMSE less than 0.04, with the highest false

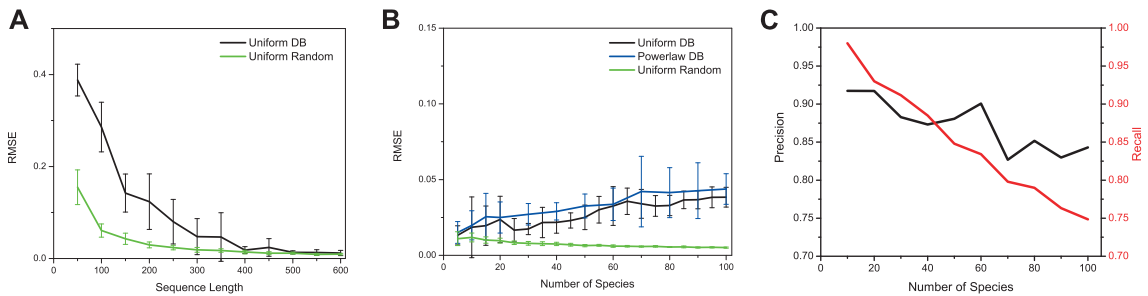


**Figure 3.3: Reconstruction of simulated mixtures.** **A.** Effect of sequence length on reconstruction performance. RMSE between the original and reconstructed frequency vectors for uniformly distributed random mixtures of  $s = 10$  species from the 16S rRNA database (black) or randomly generated sequences (green). Error bars denote the standard deviation derived from 20 simulations. **B.** Dependence of reconstruction performance on number of species in the mixture. Simulation is similar to (A) but using a fixed sequence length ( $k = 500$ ) and varying the number of species in the mixture. Blue line shows reconstruction performance on a mixture with power-law distributed species frequencies ( $v_i \sim i^{-1}$ ). **C.** Recall (fraction of sequences in the mixtures identified, shown in red) and precision (fraction of incorrect sequences identified, shown in black) of the **BCS** reconstruction of 16S rRNA the uniformly distributed database mixtures shown as black line in (B). The minimal reconstructed frequency for a species to be declared as present in the mixture was set to 0.25%.

positive reconstructed frequency (i.e. frequency for species not present in the original mixture) being less than 0.01. Using a minimal frequency threshold of 0.0025 for calling a species present in the reconstruction, the **BCS** algorithm shows an average recall of 0.75 and a precision of 0.85. Therefore, while the sequence database did not perform as well as random sequences, the 16S rRNA sequences exhibit enough variation to enable a successful reconstruction of mixtures of tens of species with a small percent of errors.

The frequencies of species in a biologically relevant mixture need not be uniformly distributed. For example, the frequency of species found on the human skin [29] were shown to resemble a power-law distribution. We therefore tested the performance of the **BCS** reconstruction on a similar power-law distribution of species frequencies with  $v_i \sim i^{-1}$ . Performance on such a power-law mixture is similar to the uniformly distributed mixture (blue and green lines in Figure 3.3.B respectively) in terms of the RMSE. A sample power-law mixture and reconstruction are shown in Figure 3.44.A,B. The recall/precision of the **BCS** algorithm on such mixtures (Figure 3.4.C) is similar to the uniform distribution for mixtures containing up to 50 species, with degrading performance on larger mixtures, due to the long tail of low frequency species.

### 3.1.4 Effect of noise on BCS solution

Experimental Sanger sequencing chromatograms contain inherent noise, and we cannot expect to obtain exact measurements in practice. We therefore turned to study the effect of noise on the accuracy of the **BCS** reconstruction algorithm. Measurement noise was modeled as additive i.i.d. Gaussian noise  $z_{ij} \sim N(0, \sigma^2)$  applied to each PSSM element in eq. (2.1). Noise is compensated for by the

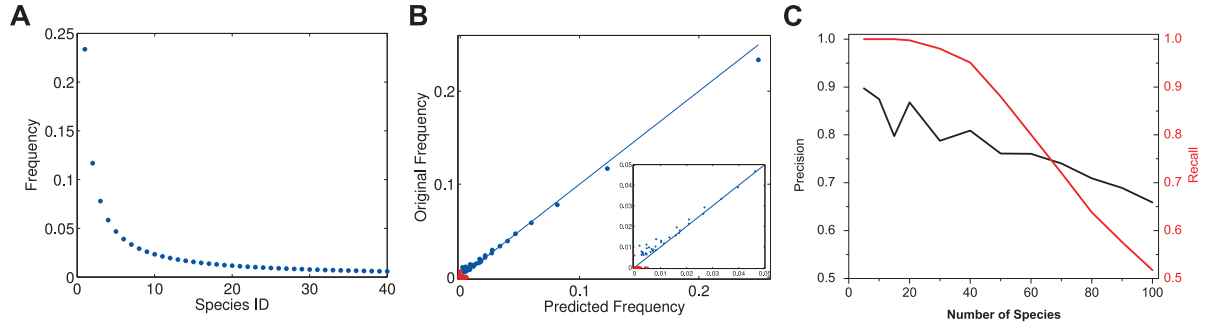


Figure 3.4: **Sample reconstruction of a power-law mixture.** **A.** Sorted frequency distribution of 40 random species following a power-law distribution with frequencies  $v_i \sim i^{-1}$ ,  $i = 1, \dots, 40$ . **B.** True vs. predicted frequencies for a sample **BCS** reconstruction for the mixture in (A) using  $k = 500$  bases of the simulated mixture. Red circles denote species returned by the **BCS** algorithm which are not present in the original mixture. **C.** Average precision (black) and recall (red) for the reconstruction of simulated mixtures with power-law distributed frequencies as in (A). The minimal reconstructed frequency for a species to be declared as present in the mixture was set to 0.17%.

insertion of the  $\ell_2$  norm into the minimization problem (see eq. (2.7)), where the factor  $\tau$  determines the balance between sparsity and error-tolerance of the solution. The effect of added random i.i.d. Gaussian noise to each nucleotide measurement is shown in Figure 3.5. The reconstruction performance slowly degrades with added noise both for the real 16S rRNA and the random sequence database.

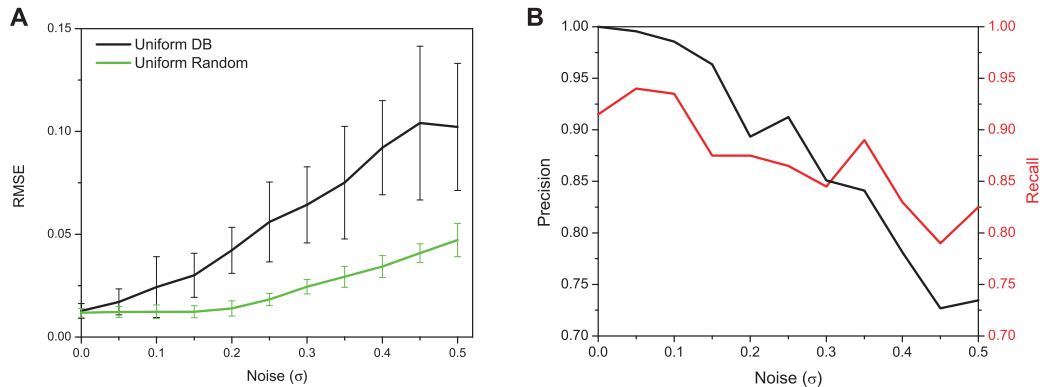


Figure 3.5: **Effect of noise on reconstruction.** **A.** Reconstruction RMSE of mixtures of  $s = 10$  sequences of length  $k = 500$  from the 16S rRNA sequence database (black) or random sequences (green), with added normally distributed noise to the chromatogram. **B.** Recall (red) and precision (black) of the 16S rRNA database mixture reconstruction shown in (A).

Using a noise standard deviation of  $\sigma = 0.15$  (which is the approximate experimental noise level - see later) and sequencing 500 nucleotides, the reconstruction performance as a function of the

number of species in the mixture is shown in Figure 3.6. Under this noise level, the **BCS** algorithm reconstructed a mixture of 40 sequences with an average RMSE of 0.07 (Figure 3.6.B), compared to  $\sim 0.02$  when no noise is present (Figure 3.3.B). By using a minimal frequency threshold of 0.006 for the predicted mixture, **BCS** showed a recall (sensitivity) of  $\sim 0.7$ , with a precision of  $\sim 0.7$  (see Figure 3.6.B), attained under realistic noise levels. To conclude, we have observed that the addition of noise leads to a graceful degradation in the reconstruction performance, and one can still achieve accurate reconstruction with realistic noise levels.

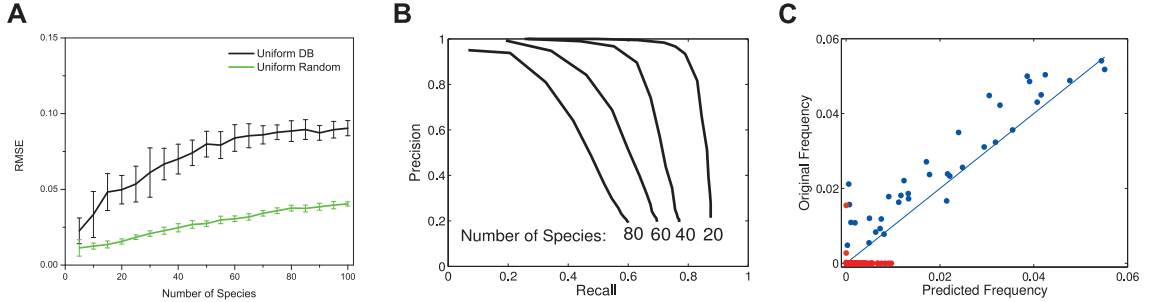


Figure 3.6: **Reconstruction with experimental noise level.** **A.** Reconstruction RMSE as a function of number of species present in the mixture. Frequencies were sampled from a uniform distribution. Noise is set to  $\sigma = 0.15$ . Sequence length is set to  $k = 500$ . Black and green lines represent 16S rRNA and random sequences respectively. **B.** Recall vs. precision curves for different number of 16S rRNA sequences as in (A) obtained by varying the minimal inclusion frequency threshold. **C.** Sample reconstruction of  $s = 40$  16S rRNA sequences from (A).

### 3.2 Reconstruction of an Experimental Mixture

We have applied our method to the problem of reconstruction of experimentally measured mixture chromatograms. This introduces a new problem of interpreting non-ideal data, mainly that Sanger sequencing chromatograms exhibit a large variability in the peak heights and positions (see Figure B.1). It has been previously shown that a large part of this variability stems from local sequence effects on the polymerase activity [41]. While for standard sequencing applications this does not pose a problem, as only the qualitative information is required (which peak shows the maxima), in our application this variability may prohibit the reconstruction. Since the measured chromatogram is a linear combination of the chromatograms of the constituting bacterial strains, variability in peak position may cause a loss of phase between the chromatogram peaks, leading to possibly overlapping peaks corresponding to different nucleotides. In order to overcome this problem, we utilize the fact that both peak position and height are local sequence dependent in order to accurately predict the chromatograms of the sequences present in the 16S rRNA database. The **CS** problem is then stated in terms of reconstruction of the measured chromatogram using a sparse subset of predicted chromatograms for the 16S rRNA database. This is achieved by binning both the predicted chromatograms and the measured mixture chromatogram into constant sized bins, and applying the **BCS** algorithm on these bins (see Methods section and Figure A.1).

A single-sequence chromatogram (measured with an ABI3730 sequencer) shows a standard de-

viation of approx. 0.26 and 1.3 for peak heights and peak-peak distances respectively (red bars in Figure B.2.B,C). In order to predict the effect of local sequence of peak height and position, we considered the preceding 5 nucleotides for each sequence position (see Methods). Statistics for the effect of each 6-mer were collected from 1000 sequencing chromatograms performed on the ABI3730 sequencer. Using this data, we can predict the peak positions and heights for a given sequence (see Figure B.2.A). The distribution of relative peak height and position errors following local sequence correction is shown in blue bars in Figure B.2.B,C, and the standard deviation is reduced to 0.15 and 0.75 for peak height and position respectively.

Using these chromatogram predictions, we tested the feasibility of the **BCS** algorithm on experimental data by reconstructing a simple bacterial population using a single Sanger sequencing chromatogram. We used a mixture of five different bacteria: (*Escherichia coli* W3110, *Vibrio fischeri*, *Staphylococcus epidermidis*, *Enterococcus faecalis* and *Photobacterium leiognathi*). DNA was extracted from each bacteria, and the 16S rRNA gene was PCR amplified using universal primers 8F and 1510R (see Methods). The resulting 16S rRNA gene was mixed in equal proportions and the mixture was sequenced using the universal 1510R primer. Data from the resulting chromatogram was used as input to the **BCS** algorithm following preprocessing steps described in the Methods section. A sample of the measured chromatogram is shown in Figure 3.7.A (solid lines). The **BCS** algorithm relies on accurate prediction of the chromatograms of each known database 16S rRNA sequence. In order to assess the accuracy of these predictions, Figure 3.7.A shows a part of the predicted chromatogram of the mixture (dotted lines) which shows similar peak positions and heights to the ones experimentally measured (solid lines). The sequence position dependency of the prediction error is shown in Figure 3.7.B. On the region of bins 125-700 the prediction shows high accuracy, with an average root square error of 0.08. The loss of accuracy at longer sequence positions stems from a cumulative drift in predicted peak positions, as well as reduced measurement accuracy. We therefore used the region of bins 125-700 for the **BCS** reconstruction.

Results of the reconstruction are shown in Figure 3.7.C. The algorithm successfully identifies three of the five bacteria (*Vibrio fischeri*, *Enterococcus faecalis* and *Photobacterium leiognathi*). Out of the two remaining strains, one (*Staphylococcus epidermidis*) is identified at the genus level, and the other (*Escherichia coli*) is mistakenly identified as *Salmonella enterica*. While *Escherichia coli* and *Salmonella enterica* show a sequence difference in 33 bases over the PCR amplified region, only two bases are different in the region used for the **BCS** reconstruction, and thus the *Escherichia coli* sequence was removed in the database preprocessing stage. When this sequence is manually added to the database (in addition to the *Salmonella enterica* sequence), the **BCS** algorithm correctly identifies the presence of *Escherichia coli* rather than *Salmonella enterica* in the mixture. Another strain identified in the reconstruction - the Kennedy Space Center clone KSC6-79 - is highly similar in sequence (differs in five bases over the region tested) to the sequence of *Staphylococcus epidermidis* used in the mixture.

## 4 Discussion

In this work we have proposed a framework for identifying and quantifying the presence of bacterial species in a given population using information from a single Sanger sequencing reaction. We have studied the amount of information present in a current database of the 16S rRNA gene sequences and the ability of using this information for unique reconstruction. Essentially, the amount of information needed for identifying the species present in the mixture is logarithmic in the database size [8, 20],

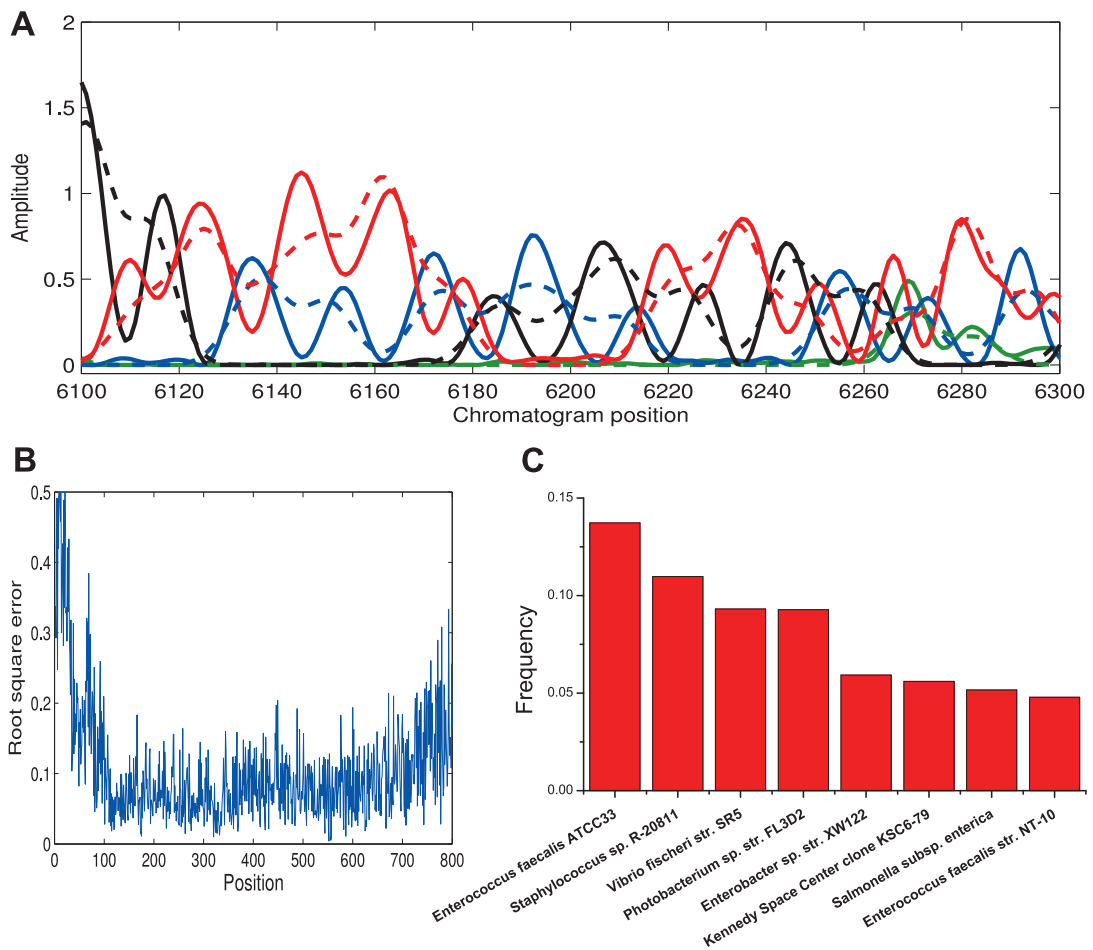


Figure 3.7: **Reconstruction of an experimental mixture.** **A.** Sample region of the mixed chromatogram (solid lines). 16S rRNA from five bacteria was extracted and mixed at equal proportion. dotted lines show the local-sequence corrected prediction of the chromatogram using the known mixture sequences. **B.** Root square distance between the predicted and measured chromatograms shown in (A) as a function of the bin position, representing nucleotide position in the sequence. Sequence positions in the range 100-700 achieved a low prediction error. **C.** Reconstruction results using the **BCS** algorithm. Runtime was  $\sim 1000$  seconds on a standard PC. Shown are the 8 most frequent species. Original strains were : *Escherichia coli*, *Vibrio fischeri*, *Staphylococcus epidermidis*, *Enterococcus faecalis* and *Photobacterium leiognathi*, with frequency 0.2 each.

as long as the number of the species present in the mixture is kept constant. Therefore, a single sequencing reaction with hundreds of bases contains in principle a very large amount of information and should suffice for unique reconstruction even when the database contains millions of different sequences. Compressed Sensing enables the use of such information redundancy through the use of linear mixtures of the sample. However, the mixtures need to be RIP in order to enable an



optimal extraction of the information. In our case, the mixtures are dictated by the sequences in the database, which are clearly dependent. While two sequences which differ in a few nucleotides clearly do not contribute to RIP, even a single nucleotide insertion or deletion completely shuffles the mixture matrix, thus enabling more efficient reconstruction through **CS**. Simulation results with noise levels comparable to the measured noise in real chromatograms indicate that this method can reconstruct mixtures of tens of species. When not enough information is present in the sequence (for example when a large number of sequences is present in the mix), the reconstruction algorithm’s performance decays gracefully, and still retains detection of the prominent species.

An important challenge we have encountered when implementing our method on experimental DNA mixtures is in the preprocessing of the Sanger sequence chromatogram. Both amplitude and position of the peaks are local-sequence dependent, and therefore corrections are needed in order to attain correct conversion of the raw chromatogram to the mixed-sequence data used as the input for the reconstruction algorithm. While the effect of local-sequence context on peak *height* can be easily incorporated into the **BCS** framework, the effect on peak *position* is more complicated to overcome. Since shifting of peak positions is independent for each sequence present in the mixture, this may result in an cumulative loss of phase in the peaks of the mixed sequence, thus preventing the calculation of the correct PSSM. We have overcome this problem by preprocessing the mixed chromatogram data (and the sequence database) at constant sized bins rather than peak-dependent nucleotide positions. In the current implementation, this preprocessing has enabled us to use approximately 600 nucleotides out of the experimental mixed chromatogram. The cumulative drift in peak position prediction is currently the limiting factor for performance of the **BCS** algorithm on experimental mixtures, as a difference of even one base position leads to a total shuffling of the PSSMs.

Since the reconstruction problem is mapped to an ordinary **CS** notation, generic **CS** tools can be applied. One problem we have faced when using the GPSR algorithm is the large memory needed for handling large problems, which forced us to remove closely similar sequences in the 16S rRNA database preprocessing step, in order to reduce the problem’s size. Developing and improving **CS** solvers is a highly active field of research, and alternative more efficient **CS** solvers such as the greedy matching pursuit approach [55] might enable tackling larger problems, without the removal of similar sequences. This has the potential to improve reconstruction results, as we have demonstrated when considering the E. Coli example, which was removed in the database preprocessing, but recovered correctly when considered as input to the **CS** algorithm. In the current implementation, the fact that bacteria have only non-negative frequencies was not explicitly enforced in eq. (2.7). Utilizing this information is known to simplify the reconstruction problem [22], and we expect it to lead to more efficient and accurate reconstruction. In the current application the mixing matrix does not fulfill the desired RIP condition as it is predetermined by the sequence database, and therefore has a high coherence which was shown to reduce performance compared to using random sequences. This coherence issue may be addressed by using novel techniques of dictionary preconditioning [50], which improve sparse signal representations in redundant dictionaries.

The proposed method can easily be extended to more than one sequencing reaction per mixture, by simply joining all sequencing results as linear constraints. Such extension can lead to a larger number of linear constraints, and thus increasing accuracy in cases such as when deciphering larger mixtures in the presence of experimental noise. For example, using an additional mixed Sanger sequencing run on the sample mixture with the 8F universal primer (instead of the 1510R primer) could enable to more easily differentiate between the *E. coli* and *S. enterica* strains, which differ mainly in the beginning of the 16S rRNA sequence. Additionally, combination of several sequencing runs can enable

reconstruction of sequences using different universal primers, thus enabling detection of multiple strains not amplified by a single universal primer. Usage of additional primers for sequencing can contribute information even when the sequenced regions overlap, since different sequences are aligned with each sequencing primer, thus creating a different shuffling of the constraints. When using only the 16S rRNA gene we cannot differentiate between species with identical 16S genes. For example, it was shown that identification via 16S rRNA sequencing enabled correct identification (up to the species level) of 95% of 328 clinical isolates [32], with the remaining 5% having non-unique sequences. In order to achieve more accurate identification of such closely related species (or sub-populations within a given species), data obtained from sequencing several genes, such as Multi-Locus Sequence Typing (MLST) [45], can also be used in the **BCS** framework. This approach can also be used when many short and inaccurate sequence fragments, which do not suffice for unique identification of each strain, are present (such as in the case of next generation sequencing methods [36]). Using a sequenced region larger than a single read length and combining the linear constraints for all the short sequences present may enable more accurate reconstruction using sparseness as the goal function.

While limited to the identification of species with known 16S rRNA sequences, the **BCS** approach may enable low cost simple comparative studies of bacterial population composition in a large number of samples.

## Acknowledgments

We thank Amit Singer, Yonina Eldar, Gidi Lazovski and Noam Shental for useful discussions, Eytan Domany for critical reading of the manuscript, Joel Stavans for supporting this research and Chaime Priluski for assistance with chromatogram peak prediction data.

## References

- [1] R.I. Amann, W. Ludwig, and K.H. Schleifer. Phylogenetic identification and in situ detection of individual microbial cells without cultivation. *Microbiol Rev*, 59(1):143–169, 1995.
- [2] F. Armougom and D. Raoult. Use of pyrosequencing and DNA barcodes to monitor variations in firmicutes and bacteroidetes communities in the gut microbiota of obese humans. *BMC Genomics*, 9(1):576, 2008.
- [3] Z. Ben-Haim, Y.C. Eldar, and M. Elad. Near-oracle performance of basis pursuit under random noise. *IEEE Trans. Signal Process*, 2009.
- [4] J. Bobin, J.L. Starck, and R. Ottensamer. Compressed sensing in astronomy. *Journal of Selected Topics in Signal Processing*, 2:718–726, 2008.
- [5] P.P. Bosshard, S. Abels, R. Zbinden, E.C. Bottger, and M. Altwegg. Ribosomal DNA sequencing for identification of aerobic gram-positive rods in the clinical laboratory (an 18-month evaluation). *Journal of Clinical Microbiology*, 41(9):4134, 2003.
- [6] J.M. Bowling, K.L. Bruner, J.L. Cmarik, and C. Tibbetts. Neighboring nucleotide interactions during DNA sequencing gel electrophoresis. *Nucleic acids research*, 19(11):3089, 1991.
- [7] E.L. Brodie, T.Z. DeSantis, J.P.M. Parker, I.X. Zubietta, Y.M. Piceno, and G.L. Andersen. Urban aerosols harbor diverse and dynamic bacterial populations. *Proceedings of the National Academy of Sciences*, 104(1):299–304, 2007.

- [8] E.J. Candes. Compressive sampling. In *Int. Congress of Mathematics*, pages 1433–1452, Madrid, Spain, 2006.
- [9] E.J. Candes. The restricted isometry property and its implications for compressed sensing. *Compte Rendus de l’Academie des Sciences*, 346:589–592, 2008.
- [10] E.J. Candes, J. Romberg, and T. Tao. Stable signal recovery from incomplete and inaccurate measurements. *Arxiv preprint math/0503066*, 2005.
- [11] E.J. Candes, M. Rudelson, T. Tao, and R. Vershynin. Error correction via linear programming. In *Annual Symposium on Foundations of Computer Science*, volume 46, pages 295–308. IEEE Computer Society Press, 2005.
- [12] E.J. Candes and T. Tao. Decoding by linear programming. *IEEE Transactions on Information Theory*, 51(12):4203–4215, 2005.
- [13] E.J. Candes and T. Tao. Near-optimal signal recovery from random projections: Universal encoding strategies? *IEEE Transactions on Information Theory*, 52(12):5406–5425, 2006.
- [14] E.J. Candes and T. Tao. The Dantzig selector: statistical estimation when  $p$  is much larger than  $n$ . *Annals of Statistics*, 35(6):2313–2351, 2007.
- [15] J.E. Clarridge III. Impact of 16S rRNA gene sequence analysis for identification of bacteria on clinical microbiology and infectious diseases. *Clinical microbiology reviews*, 17(4):840, 2004.
- [16] W. Dai, M.A. Sheikh, O. Milenkovic, and R.G. Baraniuk. Compressive sensing dna microarrays. *EURASIP Journal on Bioinformatics and Systems Biology*, 2009:oi:10.1155/2009/162824, 2009.
- [17] T.Z. DeSantis, P. Hugenholtz, N. Larsen, M. Rojas, E.L. Brodie, K. Keller, T. Huber, D. Dalevi, P. Hu, and G.L. Andersen. Greengenes, a chimera-checked 16S rRNA gene database and workbench compatible with ARB. *Applied and environmental microbiology*, 72(7):5069, 2006.
- [18] L. Dethlefsen, S. Huse, M.L. Sogin, and D.A. Relman. The pervasive effects of an antibiotic on the human gut microbiota, as revealed by deep 16S rRNA sequencing. *PLoS Biol*, 6(11):e280, November 2008.
- [19] F.E. Dewhirst, J. Izard, B.J. Paster, et al. The human oral microbiome database. 2008.
- [20] D.L. Donoho. Compressed sensing. *IEEE Transaction on Information Theory*, 52(4):1289–1306, 2006.
- [21] D.L. Donoho. For most large underdetermined systems of linear equations the minimal  $l_1$ -norm solution is also the sparsest solution. *Communications on Pure and Applied Mathematics*, 59(6):797–829, 2006.
- [22] D.L. Donoho and J. Tanner. Sparse nonnegative solution of underdetermined linear equations by linear programming. *Proceedings of the National Academy of Sciences*, 102(27):9446–9451, 2005.
- [23] M. Duarte, M. Davenport, D. Takhar, J. Laska, T. Sun, K. Kelly, and R. Baraniuk. Single-pixel imaging via compressive sampling. *IEEE Signal Processing Magazine*, 25(2):83–91, 2008.
- [24] P.B. Eckburg, E.M. Bik, C.N. Bernstein, E. Purdom, L. Dethlefsen, M. Sargent, S.R. Gill, K.E. Nelson, and D.A. Relman. Diversity of the human intestinal microbial flora. *Science*, 308(5728):1635–1638, 2005.
- [25] Y. Erlich, A. Gordon, M. Brand, G.J. Hannon, and P.P. Mitra. Compressed Genotyping. *IEEE Transactions on Information Theory*, 56(2):706–723, 2010.

- [26] B. Ewing and P. Green. Base-calling of automated sequencer traces using Phred. II. error probabilities. *Genome research*, 8(3):186, 1998.
- [27] B. Ewing, L.D. Hillier, M.C. Wendl, and P. Green. Base-calling of automated sequencer traces using Phred. I. Accuracy assessment. *Genome research*, 8(3):175, 1998.
- [28] M.A.T. Figueiredo, R.D. Nowak, and S.J. Wright. Gradient projection for sparse reconstruction: Application to compressed sensing and other inverse problems. *IEEE Journal of Selected Topics in Signal Processing*, 1(4):586–597, 2007.
- [29] Z. Gao, C. Tseng, Z. Pei, and M.J. Blaser. Molecular analysis of human forearm superficial skin bacterial biota. *Proceedings of the National Academy of Sciences*, 104(8):2927, 2007.
- [30] T. Gentry, G. Wickham, C. Schadt, Z. He, and J. Zhou. Microarray applications in microbial ecology research. *Microbial Ecology*, 52(2):159–175, 2006.
- [31] F. Guarner and J.R. Malagelada. Gut flora in health and disease. *Lancet*, 361(9356):512–519, 2003.
- [32] L. Hall, K.A. Doerr, S.L. Wohlfiel, and G.D. Roberts. Evaluation of the MicroSeq System for Identification of Mycobacteria by 16S Ribosomal DNA Sequencing and Its Integration into a Routine Clinical Mycobacteriology Laboratory. *J. Clin. Microbiol.*, 41(4):1447–1453, 2003.
- [33] M. Hamady and R. Knight. Microbial community profiling for human microbiome projects: Tools, techniques, and challenges. *Genome Research*, 19(7):1141–1152, July 2009.
- [34] M. Hamady, J.J. Walker, J.K. Harris, N.J. Gold, and R. Knight. Error-correcting barcoded primers for pyrosequencing hundreds of samples in multiplex. *Nature Methods*, 5(3):235–237, 2008.
- [35] P. Hugenholtz. Exploring prokaryotic diversity in the genomic era. *Genome Biology*, 3(2):reviews0003.1–reviews0003.8, 2002.
- [36] S.M. Huse, L. Dethlefsen, J.A. Huber, D.M. Welch, D.A. Relman, and M.L. Sogin. Exploring microbial diversity and taxonomy using SSU rRNA hypervariable tag sequencing. *PLoS Genetics*, 4(11):e1000255, 2008.
- [37] R.M. Kainkaryam and P.J. Woolf. Pooling in high-throughput drug screening. *Current opinion in drug discovery & development*, 12(3):339, 2009.
- [38] M. Keller and K. Zengler. Tapping into microbial diversity. *Nat Rev Micro*, 2(2):141–150, February 2004.
- [39] O. Kommedal, B. Karlsen, and O. Sabo. Analysis of mixed sequencing chromatograms and its application in direct 16S rDNA sequencing of poly-microbial samples. *Journal of Clinical Microbiology*, 2008.
- [40] T.T. Lin and F.J. Herrmann. Compressed wavefield extrapolation. *Geophysics*, 72, 2007.
- [41] R.J. Lipshutz, F. Taverner, K. Hennessy, G. Hartzell, and R. Davis. DNA sequence confidence estimation. *Genomics*, 19(3):417–424, February 1994.
- [42] M. Lustig, D.L. Donoho, and J.M. Pauly. Sparse mri: The application of compressed sensing for rapid MR imaging. *Magnetic Resonance in Medicine*, 58:1182–1195, 2007.
- [43] D.L. Mager, A.D. Haffajee, P.M. Devlin, C.M. Norris, M.R. Posner, and J.M. Goodson. The salivary microbiota as a diagnostic indicator of oral cancer: A descriptive, non-randomized study of cancer-free and oral squamous cell carcinoma subjects. *J Transl Med*, 3(1):27, 2005.

- [44] B.L. Maidak, J.R. Cole, T.G. Lilburn, C.T. Parker Jr, P.R. Saxman, R.J. Farris, G.M. Garrity, G.J. Olsen, T.M. Schmidt, and J.M. Tiedje. The RDP-II (ribosomal database project). *Nucleic Acids Research*, 29(1):173–174, 2001.
- [45] M.C.J. Maiden, J.A. Bygraves, E. Feil, G. Morelli, J.E. Russell, R. Urwin, Q. Zhang, J. Zhou, K. Zurth, D.A. Caugant, et al. Multilocus sequence typing: a portable approach to the identification of clones within populations of pathogenic microorganisms. *Proceedings of the National Academy of Sciences*, 95(6):3140–3145, 1998.
- [46] D. Medini, D. Serruto, J. Parkhill, D.A. Relman, C. Donati, R. Moxon, S. Falkow, and R. Rappuoli. Microbiology in the post-genomic era. *Nat Rev Micro*, 6(6):419–430, June 2008.
- [47] D.A. Nickerson, V.O. Tobe, and S.L. Taylor. PolyPhred: automating the detection and genotyping of single nucleotide substitutions using fluorescence-based resequencing. *Nucleic Acids Research*, 25(14):2745, 1997.
- [48] B.J. Paster, S.K. Boches, J.L. Galvin, R.E. Ericson, C.N. Lau, V.A. Levanos, A. Sahasrabudhe, and F.E. Dewhirst. Bacterial diversity in human subgingival plaque. *J. Bacteriol.*, 183(12):3770–3783, June 2001.
- [49] D.C. Savage. Microbial ecology of the gastrointestinal tract. *Annu Rev Microbiol*, 31:107–133, 1977.
- [50] K. Schnass and P. Vandergheynst. Dictionary preconditioning for greedy algorithms. *IEEE Transactions on Signal Processing*, 56(5), 2008.
- [51] C.L. Sears. A dynamic partnership: Celebrating our gut flora. *Anaerobe*, 11(5):247–251, 2005.
- [52] N. Shental, A. Amir, and O. Zuk. Rare Allele Detection Using Compressed Sequencing. *Nucleic Acid Research (to appear)*, 2010.
- [53] B.K. Singh, P. Millard, A.S. Whiteley, and J.C. Murrell. Unravelling rhizosphere-microbial interactions: opportunities and limitations. *Trends Microbiol*, 12(8):386–393, 2004.
- [54] Y.W. Tang, A. Von Graevenitz, M.G. Waddington, M.K. Hopkins, D.H. Smith, H. Li, C.P. Kolbert, S.O. Montgomery, and D.H. Persing. Identification of coryneform bacterial isolates by ribosomal DNA sequence analysis. *Journal of Clinical Microbiology*, 38(4):1676, 2000.
- [55] J.A. Tropp. Greed is good: Algorithmic results for sparse approximation. *IEEE Transactions on Information Theory*, 50(10):2231–2242, 2004.
- [56] J.A. Tropp. Just relax: Convex programming methods for identifying sparse signals in noise. *IEEE Transactions on Information Theory*, 52(3):1030–1051, 2006.
- [57] P.C.Y. Woo, S.K.P. Lau, J.L.L. Teng, H. Tse, and K. Yuen. Then and now: use of 16 S rDNA gene sequencing for bacterial identification and discovery of novel bacteria in clinical microbiology laboratories. *Clinical Microbiology and Infection*, 14(10):908–934, 2008.

# Appendix

## A Chromatogram Preprocessing

In order to apply the **BCS** algorithm on the experimentally measured mixture chromatogram, several preprocessing steps are required. The purpose of the chromatogram preprocessing step is to convert the measured chromatogram to a PSSM representing the frequency of each base at each position in the mixture (see Figure A.1.A).

The input to the chromatogram preprocessing is the measured chromatogram, consisting of four fluorescent trace vectors  $\mathbf{a}, \mathbf{c}, \mathbf{g}, \mathbf{t}$ , where for example  $\mathbf{a}_p$  represents the signal intensity for nucleotide 'A' at the  $p$ 's position along the chromatogram, where each position is represented by one pixel in the chromatogram image. The value  $p$  corresponds roughly to the timing of the sequencing reaction, with a resolution of approximately a dozen points per nucleotide, thus  $p$  runs from 1 to  $\sim 12k$ .

In a typical Sanger sequencing reaction, the chromatogram peak heights decrease at higher  $p$  values (nucleotides further in the sequence which were sequenced later in the sequencing reaction) due to depletion of the dideoxynucleotides. To overcome this long-scale decrease in signal amplitude, prior to the binning step, the amplitude at each position was normalized by division with average total peak height in a  $\sim 50$  base-pair (bp) region around each position (see step 1 in the algorithm description below).

The resulting vectors after the normalization step are binned into constant sized bins, and the sum of intensity values of each bin is computed for the four different nucleotides. Then, we take square root of this sum for the four different nucleotides for the  $i$ 'th bin as the  $i$ 'th column in the output  $4 \times k$  PSSM. The square root is used rather than the sum as this was shown to decrease the effect of large outliers. The resulting  $4 \times k$  PSSM is used as input to the **BCS** reconstruction. Formally, the preprocessing algorithm is described below:

**Algorithm:** Chromatogram Preprocessing

**Input:**  $(\mathbf{a}, \mathbf{c}, \mathbf{g}, \mathbf{t})$  - four fluorescent trace vectors

**Output:**  $P = (a, c, g, t)^t$  - a PSSM representing nucleotide frequencies

1. Normalize the chromatogram amplitude:

$$\mathbf{a}_p = \frac{50 \cdot 12 \cdot \mathbf{a}_p}{\sum_{q=-25 \cdot 12}^{25 \cdot 12} (\mathbf{a}_{p+q} + \mathbf{c}_{p+q} + \mathbf{g}_{p+q} + \mathbf{t}_{p+q})} \quad (\text{A.1})$$

and similarly for  $\mathbf{c}_p, \mathbf{g}_p$  and  $\mathbf{t}_p$ .

2. bin into constant sized bins, average bin values and apply square root transformation:

$$a_i = \sqrt{\sum_{p=12i}^{12i+11} \mathbf{a}_p}, \quad i = 1 \dots k \quad (\text{A.2})$$

and similarly for  $c_i, g_i, t_i$ .

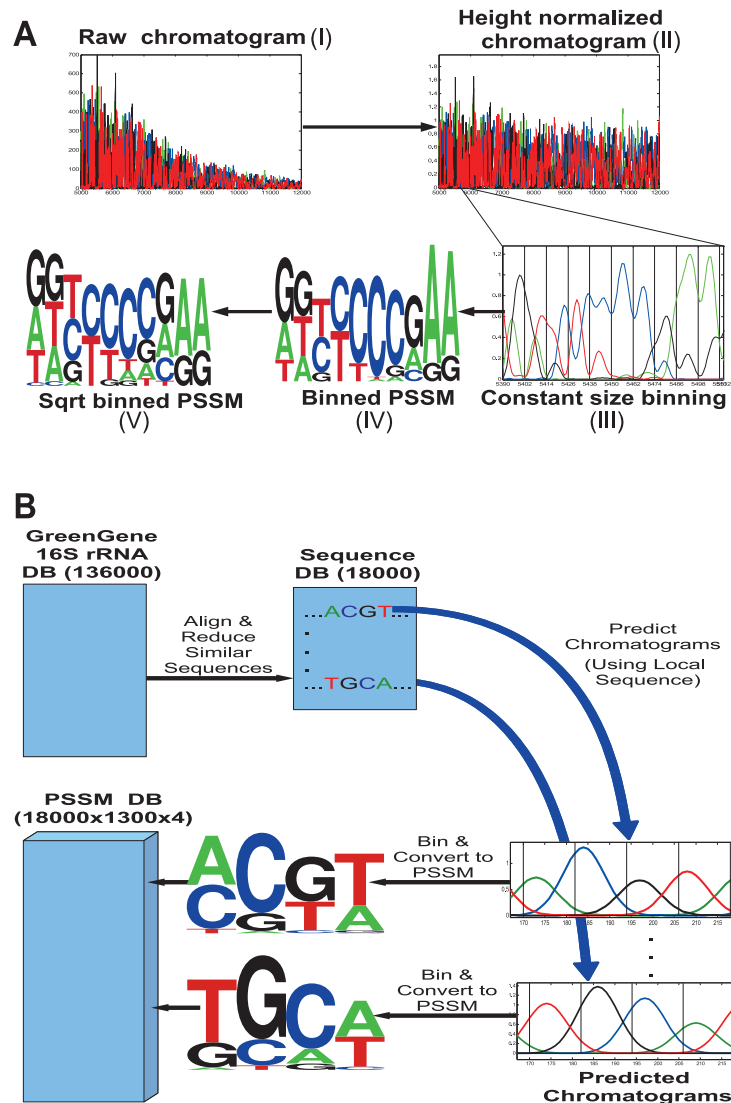


Figure A.1: **Preprocessing steps A.** Preprocessing of the experimental chromatogram. The result of the Sanger-sequencing of a bacterial mixture (I) is normalized by division with a  $\sim 1000$  pixel total intensity running average to compensate for the peak amplitude decrease. The resulting chromatogram (II) is binned into constant sized bins (sample section shown in III), and the resulting PSSM (sample section shown in IV) is further square-root transformed to obtain the final experimental PSSM (sample section shown in V). **B.** Preprocessing of the 16S rRNA sequence database. Sequences are first aligned and similar sequences are removed. Then, a predicted chromatogram is generated for each sequence in the database, based on local sequence statistics collected from a training set. Finally, the predicted chromatograms are binned into constant sized binned and the resulting PSSMs are further square-root transformed in similar to (A), to produce the final PSSMs which are stored in the database.

## B Database Preprocessing

The purpose of the Database Preprocessing scheme is to produce predicted PSSMs for all 16S rRNA sequences in the database (see Figure A.1.B). These predicted PSSMs are used later in the reconstruction algorithm as 'basis vectors' whose linear combination with the appropriate coefficients gives the PSSM obtained from observed mixed chromatogram, as described in the previous section. An important intermediate stage in obtaining the predicted PSSMs is generation of predicted chromatograms for the database sequences. When generating predicted chromatograms we take into account local sequence context - the estimation of this sequence context effects requires a training set of real chromatograms from known sequences from which chromatogram peak height and positions statistics are computed as a preliminary step. The database preprocessing therefore contains two steps:

1. A preliminary step: Compute local-sequence adjusted chromatogram statistics.  
Here we use a training set  $S'$  of known sequences and their chromatograms as input and compute tables  $H$  and  $P$  representing chromatogram peak heights and positions, respectively, for different local-sequence contexts.
2. Database PSSMs Generation step: Generate a database of predicted PSSMs.  
Here the input is a set  $S$  of  $N$  sequences and the pre-computed tables  $H$  and  $P$ . The sequence input and tables are used to determine peak heights and positions and compute a set of  $N$  chromatograms of the form  $(\mathbf{a}, \mathbf{c}, \mathbf{g}, \mathbf{t})$ , one for each sequence in the database. These chromatograms are then further processed to get predicted PSSMs. This step is illustrated in Figure A.1.B.

After performing these two steps, an additional alignment step is required to match the start of the measure and predicted chromatograms.

### B.1 Preliminary Step: Compute local-sequence adjusted chromatogram statistics

In the course of the Sanger sequencing process, both the polymerase specificity for incorporating deoxynucleotides over dideoxynucleotides and the fragment mobility depend on sequence local to the incorporation point. Therefore for each nucleotide in the DNA fragment being sequenced, its corresponding chromatogram peak height  $a$  and position  $b$  are affected by the preceding nucleotides [41]. In order to predict and correct for the effect of local sequence context on the resulting chromatogram, we collected statistics from a training set  $S'$  of 1000 sequencing runs performed on an ABI3730 machine. Runs were obtained from various Sanger sequencing experiments performed by different labs and for different organisms thus presenting us with a diverse genomic training set. The average length of the runs was approximately 800 base-pairs. Chromatogram heights were normalized to overcome the long scale amplitude decrease (as described in the Chromatogram Preprocessing section) and chromatogram peaks were identified. We use  $p_{i,j}$  and  $h_{i,j}$  to denote the position and height of the  $j$ -th nucleotide in the  $i$ -th sequence, respectively (we have chosen the top peak out of the four traces representing different bases - since each chromatogram represented a single sequence, these peaks were in most cases clearly higher and distinguishable from the three other peaks).

We have modeled the local sequence context by looking at the 5 nucleotides preceding each nucleotide, giving us  $4^6 = 4096$  different unique 6-mers, each representing a possible nucleotide and the 5 nucleotides preceding it. For each unique 6-mer, we have searched for all of its occurrences in the 1000 sequences, and averaged the peak height and position data of the last nucleotide over all



such occurrences in the 1000 sequences analyzed. We have used 6-mers as this gives the maximal context length for which we had sufficient statistics to collect for each bin (approximately 200 instances per bin, on average) - it is possible that smaller context is sufficient for accurate prediction of chromatogram heights. More formally, for a given kmer  $\alpha = (\alpha_1, \dots, \alpha_6)$ , we have computed  $H(\alpha)$  and  $P(\alpha)$  as follows. The peak height statistic  $H(\alpha)$  measures the corresponding local-averaged peak heights:

$$H(\alpha) = \frac{\sum_{i,j} 1_{\{\alpha_1=S'_{i,j-5}, \dots, \alpha_6=S'_{i,j}\}} h_{i,j}}{\sum_{i,j} 1_{\{\alpha_1=S'_{i,j-5}, \dots, \alpha_6=S'_{i,j}\}}} \quad (\text{B.1})$$

For peak position  $P(\alpha)$ , we first computed the relative peak-peak distance for each position:

$$d_{i,j} = \frac{p_{i,j} - p_{i,j-1}}{\sum_{j=2}^k p_{i,j} - p_{i,j-1}}. \quad (\text{B.2})$$

Then, we measured the average relative peak-peak distance between the current peak and the previous peak:

$$P(\alpha) = \frac{\sum_{i,j} 1_{\{\alpha_1=S'_{i,j-5}, \dots, \alpha_6=S'_{i,j}\}} d_{i,j}}{\sum_{i,j} 1_{\{\alpha_1=S'_{i,j-5}, \dots, \alpha_6=S'_{i,j}\}}} \quad (\text{B.3})$$

The results were the final peak height and position tables  $H$  and  $P$  respectively, each of size  $4096 (= 4^6)$  (available on the article website). While the average height and position were 1 (as was ensured by our normalizations), there was significant variability in height and position according to sequence context, with height values  $H$  typically in the range  $\sim 0.5 - 1.3$  and position values  $P$  in the range  $\sim 0.8 - 1.2$  (see Figure B.1). An additional sequence-independent non-linearity in the peak position was observed in the chromatograms studied, where distance between consecutive peak increases as we move further along the chromatogram. This was accounted for by fitting an additional linear model based only on the nucleotide sequence position, giving an additional parameter of  $\beta = 0.00036$  representing increase in peak-peak distance with each position (see next section in eq. (B.4)).

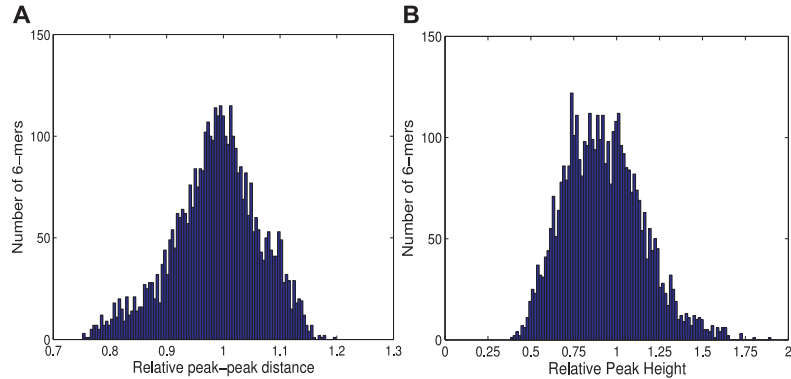


Figure B.1: **Local-sequence effect on chromatogram peak height and position.** **A.** Distribution of average normalized peak-peak distances for the 4096 sequence 6-mers. **B.** Distribution of normalized peak heights for the 4096 sequence 6-mers. Both distributions show a rather wide spread around one, showing that local sequence context has a significant effect on peak height and position.

## B.2 Database PSSMs Generation step: Generate a database of predicted PSSMs.

The input for this step is the database sequence matrix  $S$  and the output is a set of PSSMs  $(a, c, g, t)^t$ , one for each sequence  $S_i$  in the database. The database processing scheme is applied only once to the database and the predicted PSSMs are stored and can be used for any new mixture sample obtained. It is applied to each sequence in the database independently.

For every nucleotide in the database, we estimated its chromatogram peak height and peak-peak distance as:

$$a_{i,j} = H(L_{i,j}), \quad b_{i,j} = b_{i,j-1} + P(L_{i,j}) + \beta j \quad (\text{B.4})$$

where  $L_{i,j} = (S_{i,j-5}, \dots, S_{i,j})$  denotes the local 6-mer sequence context of nucleotide  $j$  in the  $i$ -th sequence ( $L_{i,j} \in 1\dots 4^6$ ). The parameter  $\beta = 0.00036$  represents the increase in peak-peak distance per position as we move further along the sequence.

In order to generate a chromatogram trace for a given sequence, each peak was modeled as a Gaussian centered at the peak position and with height equal to the peak height. Thus, for every nucleotide in a sequence, a corresponding peak was created in the chromatogram using the Gaussian peak function

$$f_{i,j}(x) = a_{i,j} e^{-\frac{(x-b_{i,j})^2}{2c^2}} \quad (\text{B.5})$$

The widths of the chromatogram Gaussian peaks were approximated by using a constant peak width obtained by setting  $c = 0.4$ . A chromatogram was generated for each sequence by summing the values of obtained  $f_{i,j}$  over all nucleotides. Each  $f_{i,j}$  was evaluated for  $x$  values equally spaced in the range  $[0, k]$ , at a resolution of  $1/12$  thus giving  $12k$  different  $x$  values  $x_1, \dots, x_{12k}$ . Each  $f_{i,j}$  contributed to the sum only for the trace of the corresponding base in the sequence, and for the other three bases the contribution to the sum was zero. That is, the trace vector for the nucleotide 'A' for the  $i$ -th sequence was computed as:

$$\mathbf{a}_p = \sum_j f_{i,j}(x_p) 1_{\{S_{i,j}='A'\}} \quad (\text{B.6})$$

and similarly for the other three nucleotides. The resulting predicted chromatograms were binned using a constant bin size of 1 and transformed via square root, in similar to the chromatogram preprocessing step in eq. (A.2), to give a PSSM database with one PSSM for each sequence in  $S$ .

## B.3 Alignment of Predicted and Measured Chromatograms

Sanger-sequencing chromatograms display an initial region ( $\sim 100$  bases) which is highly noisy and therefore unusable. We are therefore faced with the problem of correctly aligning the initial bin position in the measured chromatogram and the bin positions of the predicted chromatograms. This was solved by trying the **BCS** reconstruction for different initial bin offsets in the measured chromatogram, and selecting for the offset with the lowest reconstruction root square distance (see Figure B.3.A). This reconstruction root square distance is calculated as the difference between the measured chromatogram and the predicted chromatogram based the reconstructed species frequencies. To verify the validity of this criterion, we also compared the average distance between the measured chromatogram and the predicted mixture chromatogram obtained using the known mixture composition (see Figure B.3.B), using various offsets for the measured chromatogram binning. Both methods obtained an identical offset, which was used in the reconstruction.

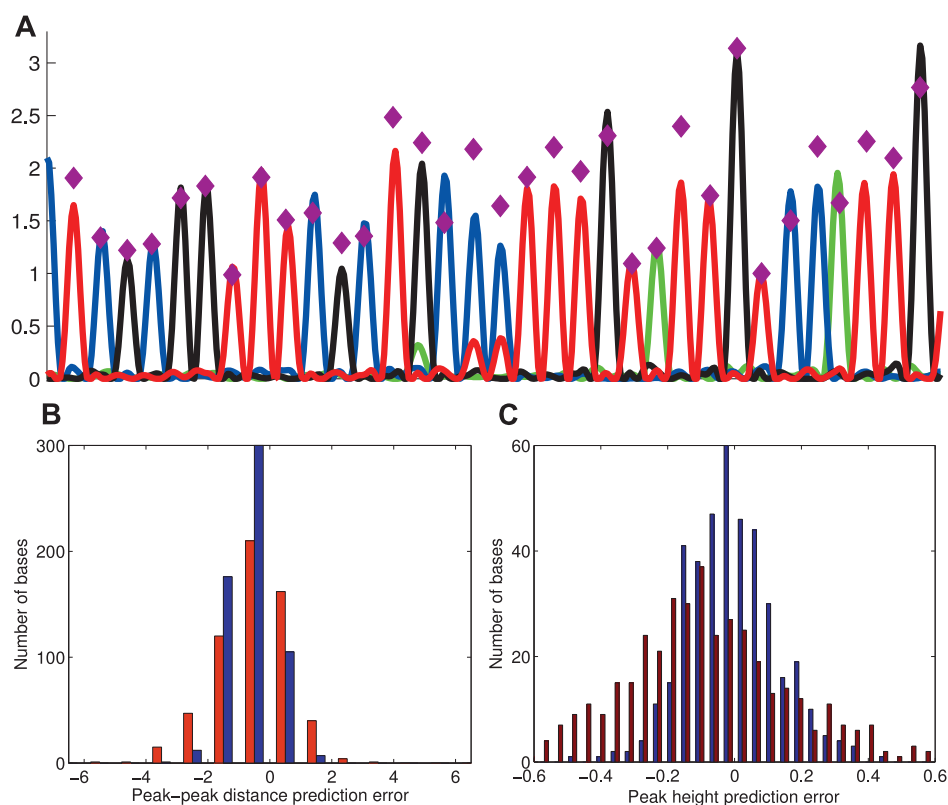


Figure B.2: **Effect of local sequence on chromatogram peak heights and positions.** **A.** Sample sequenced chromatogram and prediction (magenta circles) of peak heights and positions based on local (6-mer) sequence. **B.** Distribution of peak-peak distance differences between predicted and measured peak positions before (red) and after (blue) correction for local sequence effects. The average peak-peak distance is  $\sim 12$  pixels. **C.** Distribution of distance between predicted and measured peak heights before (red) and after (blue) correction for local sequence effects. Employing local sequence context improves both height and positions predictions.

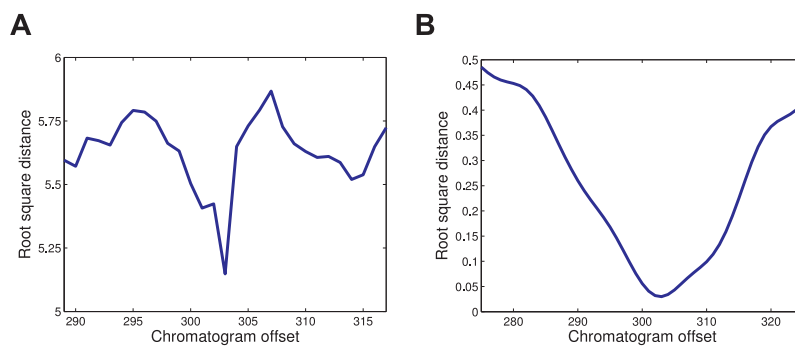


Figure B.3: **Determination of chromatogram offset.** **A.** Root square distance between measured chromatogram and the chromatogram predicted from the **BCS** reconstruction. Minimal value is obtained when position 1 in the measured chromatogram is aligned to position 304 in the database. **B.** Root square distance between measured chromatogram and the chromatogram predicted using the known composition of the five species in the mixture. Minimal value is obtained when position 1 in the measured chromatogram is aligned to position 304 in the database.